Design of Aircraft Wings Subjected to Gust Loads: A Safety Index Based Approach

J.-S. Yang*
Aerostructures, Inc., Arlington, Virginia 22202
and
E. Nikolaidis†
Virginia Polytechnic Institute and State University, Blacksburg, Virginia 24061

A method for system reliability based design of aircraft wings is presented. The advanced first-order, second-moment (AFOSM) method is employed in evaluating reliability. A wing of a commuter aircraft designed by the FAA regulations is compared to one designed by system reliability optimization. Two cases are considered for which the correlation between failure modes is neglected or is accounted for, respectively. The results demonstrate the potential of system reliability optimization and the benefits from employing the AFOSM method. Furthermore, they allow us to identify the limitations of simple methods utilizing the first-order Ditlevsen bounds for evaluating system reliability and to assess the advantages of more sophisticated system reliability based methods that account for the correlation between the failure modes. It is shown that, if a penalty function method is employed for optimization, the upper Ditlevsen bound can be used to approximate the system reliability without encountering any problems due to the discontinuity of the derivatives of the constraints.

Introduction

AIRCRAFT structural design is still conducted using deterministic or quasiprobabilistic methods.[1] In both cases the safety of the individual structural components rather than the overall system safety is considered. Furthermore, the effects of the structural redundancy on the overall reliability are often ignored. The resulting designs are inefficient in terms of weight, or they may even be unsafe.

Recently developed system reliability methods for analysis of structural safety[2] take into account structural redundancy and yield a safety measure of the overall structure viewed as a system. Application of system reliability principles is expected to overcome the drawbacks of currently used procedures for structural design.

The number of publications on structural optimization based on system reliability is still limited. The reason is the complexity of the procedure and the excessive amount of computational effort required for evaluating system reliability. F. Moses was among the first to study structural system reliability based optimization. A technique for optimal design of a structure with a prescribed safety level was presented in Ref. 3. Although the technique was based on some rather restrictive assumptions on the statistical correlation of the loads and the strengths of the structural members, it was demonstrated that use of system reliability results in a design that is considerably different from that from deterministic or element reliability based optimization.

Thoft-Christensen and Sorensen[4,5] established a procedure for system reliability based optimization for framed structures, using the beta-unzipping method[2] for estimating system reliability. The sensitivity derivatives of the safety index of each failure element or of the system were calculated using semianalytical formulas. Feng and Moses[6] derived an optimality criterion for sizing the components of framed structures that satisfy a system reliability constraint. This criterion, which is a special case of the Kuhn-Tucker conditions, states that, at the optimum, the sensitivity derivatives of the system reliability with respect to the weight of the structural members are all equal. An algorithm for structural optimization, based on the preceding criterion, was described in the same reference. The effect of the requirement for high structural redundancy on the final design, when using system reliability optimization, was studied by the same authors.[7] It was concluded that, for structures with low degree of indeterminancy, the requirements for high redundancy and low weight or cost are opposing each other.

Frangopol[8] presented an interactive reliability-based computer-aided design (CAD) optimization procedure for plastic framed structures that accounts for the correlation between various loads and strengths. Since the procedure is interactive, it gives an insight into the reliability optimization problem. A technique for sensitivity analysis of the optimum design was presented by the same author.[9] It was shown that the optimum solution can be more sensitive to the correlation between the strengths of the structural members than to the method employed to evaluate the failure probability.

Rao[10] used element reliability optimization to design an aircraft wing subjected to gust and landing loads. The constraints for the safety of the wing were evaluated by the first-order, second-moment method. An element reliability optimization approach for aircraft wings design that accounts for dynamic effects was presented by Hajela and Bach.[11,12] The design constraints considered correspond to the first excursion and fatigue failure modes. The question of combining different loads applied to the aircraft was also addressed in the last two references. However, no comparison between the results of the deterministic and the probabilistic approach that would lead to meaningful conclusions on the potential of the probabilistic approach was made. Furthermore, element reliability optimization does not allow to fully exploit the advantages of probabilistic design.

Yang et al.[13] presented a probabilistic method for system reliability based design of aircraft wings subjected to gust loads. The level III method was used to evaluate the probability of failure of each segment of a model representing the aircraft wing. This method calculates the failure probability by integrating the joint probability density function of the random load and strength variables over the failure region. The numerical integration required made the computational cost excessive. Although the method employed demonstrated

Received Sept. 6, 1989; revision received Feb. 24, 1990.

*Project Engineer, formerly Graduate Research Assistant, Virginia Polytechnic Inst., Department of Aerospace and Ocean Engineering.

†Assistant Professor, Department of Aerospace and Ocean Engineering. Member AIAA.

the benefits from reliability optimization, and indicated some trends in distributing material in optimal design, its high computational cost did not allow the consideration of the statistical correlation between different failure modes. The high computational cost required by the level III method becomes a major problem in real-life designs where many random variables are involved.

The AFOSM, which can be used to estimate reliability, is reasonably accurate and considerably cheaper than the level III method. On the other hand, it is more accurate than the mean value, first-order, second-moment method (MVFOSM).[14] Therefore, the AFOSM method is a good compromise between the requirements for high accuracy and computational efficiency. We can employ the AFOSM method to circumvent the aforementioned shortcomings of the reliability optimization procedure presented in Ref. 13.

The objective of this paper is to demonstrate the potential of system reliability based optimization, in conjunction with the AFOSM method, to reduce the weight and increase the safety of aircraft structures. First we present a methodology for system reliability design of an aircraft wing. The design procedure consists of the following steps:

1) development of a design-oriented model of the wing;
2) development of a statistical model for the gust loads;
3) estimation of element reliability of the wing;
4) estimation of the system reliability of the wing;
5) evaluation of the derivatives of the system reliability with respect to the design variables; and
6) formulation and solution of the optimization problem.

In order to illustrate the advantages of the proposed design methodology, we designed the wing of a commuter aircraft following the FAA regulations. This structure was compared to two wings designed using system reliability optimization. The first design has the same probability of failure as the deterministic one, whereas the other has the same weight. It was shown that system reliability optimization dramatically improves the design of aircraft structures.

System Reliability of the Wing

Wing Model

A simple box beam consisting of 12 segments was used to model the wing. The wing planform and the box profile are shown in Fig. 1.

The reliability analysis of the wing is based on the following assumptions:

1) The flanges take normal stress only, and the webs take the shear stress.
2) The loads due to gusts are treated as static.

Although these assumptions are not always realistic, they are acceptable in the context of our study. Indeed, the objective is to demonstrate the potential of reliability optimization and to identify trends and not to design a real-life structure. According to the preceding assumptions, the wing was viewed as a system consisting of 24 failure subsystems connected in series. The first 12 subsystems represent the flanges of each beam segment, and the last 12 represent the webs. Thus, we have 24 failure modes, of which the first 12 correspond to bending and the rest correspond to shear.

Statistical Model of the Gust Loading

Assuming that the upcrossings of a threshold by the gust factor constitute a Poisson process, the probability distribution function of the maximum value of the gust load factor $F_L(l)$, encountered over a time period of length T, is

$$F_L(l) = \exp[-N(l)T] \tag{1}$$

where

$$N(l) = N_0\left\{p_1 \exp\left(\frac{-l}{Ab_1}\right) + p_2 \exp\left(\frac{-l}{Ab_2}\right)\right\} \tag{2}$$

and where

L = random variable representing the gust load factor
$N(l)$ = average up-crossing rate of level l by the gust load factor
T = lifetime of the aircraft
N_0 = up-crossing rate of level 0 by the gust load factor
A = ratio of the standard deviation of load factor to that of the gust load
b_1 = standard deviation of stormy gust speed
b_2 = standard deviation of nonstormy gust speed
p_1 = probability of encountering stormy gust
p_2 = probability of encountering nonstormy gust
l = realization of the random variable L

FAA regulations[1] recommend values for parameters p_1, p_2, b_1, and b_2, and A and N_0 are evaluated by using the method suggested in Ref. 15. The lifetime of the aircraft is assumed to be 30,000 h.

The statistical model in Eqs. (1) and (2) would be valid for the case that the airplane was scheduled to fly at a constant speed and altitude. Therefore, mission profiles consisting of different flying conditions were assumed to obtain the combined effects from gust loads as described in Ref. 13.

The Weibul distribution function was used to fit the numerically obtained original distribution function of the gust load factor. The fitted Weibul distribution and density functions are

$$F_L(l) = \exp\left[-\left(\frac{l}{\gamma}\right)^{\alpha}\right] \tag{3}$$

and

$$f_L(l) = \frac{\alpha x^{\alpha-1}}{\gamma^{\alpha}} \exp\left[-\left(\frac{l}{\gamma}\right)^{\alpha}\right] \tag{4}$$

respectively. The values of the coefficients involved in Eqs. (3) and (4) are $\alpha = 2.2567$ and $\gamma = 1.4616$.

Element Reliability Analysis

The safety of each failure subsystem is quantified by its safety index, which is the final product from the application

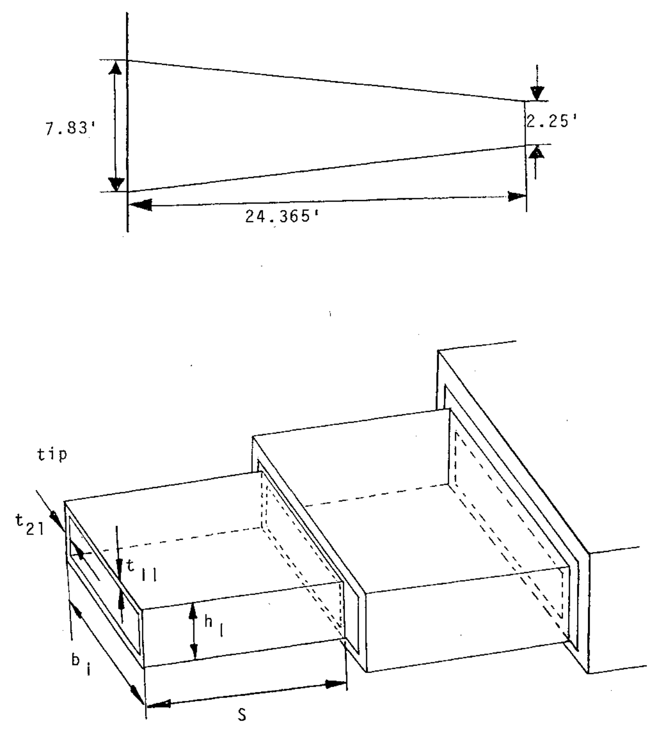

Fig. 1 Wing planform and box beam profile.

of the AFOSM method. This method is summarized as follows. First, the limit state function is defined. This function depends on the values of the random variables, and it becomes negative when the structure fails and positive when it survives. The limit state function is considered in the reduced space of the random variables. The surface corresponding to the zero value of the function is the boundary between survival and failure, and the point on this surface that is closest to the origin is called the design point. The AFOSM method locates this point through an iterative procedure. The distance from the design point to the origin is called the safety index, and it is usually denoted β. For limit state functions that are not highly nonlinear, the probability of failure can be approximated with good accuracy as follows:

$$P_f \cong \Phi(-\beta) \tag{5}$$

where P_f is the probability of failure, and Φ the probability distribution function of a standard normal random variable.

If the limit state function is highly nonlinear, the second-order reliability method (SORM), which approximates the failure surface by a second-degree polynomial, can be used to improve the accuracy.[16] In our study the limit state functions are mildly nonlinear. Indeed, the AFOSM method yields almost identical results with Ref. 13, which uses the level III method to solve the same problem.

The limit state functions are expressed as follows:

$$R_s - s_{si} = 0, \qquad i = 1, 2, \ldots, 12 \tag{6}$$

for shear failure, and

$$R_b - s_{bi} = 0, \qquad i = 1, \ldots, 12 \tag{7}$$

for bending failure.

In these equations R_s is the shear strength, R_b the tensile strength, s_{si} the shear stress, and s_{bi} the bending stress. The subscript i denotes the segment number. It is 1 for the segment at the wing tip and 12 for the segment at the root.

The bending and shear stresses can be calculated by using beam theory. They are proportional to the load factor according to the following equations:

$$s_{si} = c_{si}(L + 1) \tag{8}$$

and

$$s_{bi} = c_{bi}(L + 1) \tag{9}$$

where c_{si} is the constant in the linear relation between the shear stress and the load factor, and c_{bi} is the constant in the linear relation between the bending stress and the load factor.

R_s and R_b were assumed to be normal random variables. The reduced strengths variables are defined as

$$R_s' = \frac{R_s - \mu_s}{\sigma_s} \tag{10}$$

$$R_b' = \frac{R_b - \mu_b}{\sigma_b} \tag{11}$$

where μ_s is the mean value of shear strength, μ_b the mean value of tensile strength, σ_s the standard deviation of shear strength, and σ_b the standard deviation of tensile strength.

Since L is not normally distributed, we need to transform it to a standard Gaussian random variable in order to use the AFOSM method. The application of the Rosenblatt transform[17] to our problem yields

$$L = F^{-1}[\Phi(L')] \tag{12}$$

where L' is the reduced random variable of the gust load factor.

Therefore, the limit state functions become

$$R_s'\sigma_s + \mu_s - c_{si}(F^{-1}[\Phi(L')] + 1) = 0, \qquad i = 1, \ldots, 12 \tag{13}$$

and

$$R_b'\sigma_b + \mu_b - c_{bi}(F^{-1}[\Phi(L')] + 1) = 0, \qquad i = 1, \ldots, 12 \tag{14}$$

for the shear and bending failure, respectively. Consequently,

$$\beta = \min \sqrt{R_s'^2 + L'^2} \tag{15}$$

for shear failure, and

$$\beta = \min \sqrt{R_b'^2 + L'^2} \tag{16}$$

for bending failure.

The calculation of the safety indices for the shear and bending failure modes is a minimization problem with Eqs. (15) and (16) as objective functions and with Eqs. (13) and (14) as constraints.

System Reliability Analysis

The individual failure probabilities of each failure subsystem were combined to evaluate the system probability of failure. The exact evaluation of the failure probability is a formidable task that requires knowledge of the joint probabilities corresponding to all combinations of the failure modes.

Fortunately, we can approximate the system failure probability by various bounds that can be evaluated inexpensively. In this study we selected Ditlevsen's first- and second-order upper bounds.

First-Order Upper Bound

The system probability of failure can be approximated by the first-order upper bound as follows:

$$P_f \cong \sum_{k=1}^{24} P(e_k) \tag{17}$$

or, equivalently,

$$\Phi(-\beta_s) \cong \sum_{k=1}^{24} \Phi(-\beta_k) \tag{18}$$

where P_f is the system probability of failure, β_s the system safety index, and e_k the event that the kth failure mode occurs.

Consequently,

$$\beta_s \cong -\Phi^{-1}\left[\sum_{k=1}^{24} \Phi(-\beta_k)\right] \tag{19}$$

Second-Order Upper Bound

The probability of failure can be more accurately approximated by using Ditlevsen's second-order upper bound[18] as follows:

$$P_f \approx \sum_{k=1}^{24} P(e_k) - \sum_{k=2}^{24} \max_{j<k} P(e_k \cap e_j) \tag{20}$$

where

$$P(e_k \cap e_j) \cong \Phi_2(-\beta_k, -\beta_j, \rho_{kj}) \tag{21}$$

and where Φ_2 is the bivariate normal distribution function, and ρ_{kj} the correlation coefficient between the limit state functions corresponding to the kth and the jth modes.

Consequently,

$$\beta_s \approx -\Phi^{-1}\left[\sum_{k=1}^{24} \Phi(-\beta_k) - \sum_{k=2}^{24} \max_{j<k} \Phi_2(-\beta_k, -\beta_j, \rho_{kj})\right] \tag{22}$$

Obviously, the second-order bound accounts for the statistical correlation between failure modes, whereas the first-order bound neglects it.

System Reliability Optimization

Optimization Formulations

Two system reliability optimization formulations, minimum weight and maximum safety, were investigated.

Minimum Weight Optimization

The objective here is to minimize the weight of the wing:

$$W = \sum_{i=1}^{12} 2\bar{\rho}s(b_i t_{1i} + h_i t_{2i}) \tag{23}$$

where
i = beam segment number
b_i = width of the beam segment
h_i = height of beam segment
s = length of beam segment
t_{1i} = thickness of flange
t_{2i} = thickness of web
W = weight of the wing
$\bar{\rho}$ = material density

The constraint is

$$\beta_s \geq \beta_p \tag{24}$$

where β_p is the prescribed safety index.

Maximum Safety Optimization

The objective here is to maximize the safety index,

$$\beta_s \tag{25}$$

The constraint is

$$W \leq W_p \tag{26}$$

where W_p is the prescribed weight. We can employ any standard algorithm for constrained optimization to solve these problems.

Calculation of Constraint Derivatives

The sensitivities of β_s with respect to the design variables can be evaluated semianalytically as follows.

The limit state function of failure element k can be written as

$$g_k(\boldsymbol{u},\boldsymbol{t}) = 0 \tag{27}$$

where $\boldsymbol{u}$ is the normalized vector of random variables, and $\boldsymbol{t}$ the design variable vector.

It can then be shown[19] that

$$\frac{\partial \beta_k}{\partial t_j} = \frac{1}{\|\nabla_u g_k(\boldsymbol{u}^\times,\boldsymbol{t})\|} \frac{\partial g_k(\boldsymbol{u}^\times,\boldsymbol{t})}{\partial t_j} \tag{28}$$

where $\boldsymbol{u}^\times$ is $\boldsymbol{u}$ evaluated at the design point, and $\nabla_u g_k(\boldsymbol{u}^\times,\boldsymbol{t})$ the gradient of g_k with respect to $\boldsymbol{u}$ evaluated at the design point.

The gradient of g_k can be calculated using Eqs. (13) and (14). Therefore,

$$\|\nabla_u g_k(\boldsymbol{u}^\times,\boldsymbol{k})\| = \sqrt{\left(\frac{\partial g_k}{\partial L'}\right)^2 + \left(\frac{\partial g_k}{\partial R_s'}\right)^2} \tag{29}$$

for failure in shear, and

$$\|\nabla_u g_k(\boldsymbol{u}^\times,\boldsymbol{t})\| = \sqrt{\left(\frac{\partial g_k}{\partial L'}\right)^2 + \left(\frac{\partial g_k}{\partial R_b'}\right)^2} \tag{30}$$

for failure in bending.

From Eq. (12) it is observed that

$$\frac{\partial L}{\partial L'} = \frac{\phi(L')}{f(L)} \tag{31}$$

where ϕ is the probability density function of a standard normal random variable.

Therefore,

$$\frac{\partial g_k}{\partial L'} = -\frac{c_{sk}\phi(L')}{f(L)} \tag{32}$$

for failure in shear,

$$\frac{\partial g_k}{\partial L'} = -\frac{c_{bk}\phi(L')}{f(L)} \tag{33}$$

for failure in bending,

$$\frac{\partial g_k}{\partial R_s'} = \sigma_s \tag{34}$$

and

$$\frac{\partial g_k}{\partial R_b'} = \sigma_b \tag{35}$$

Since R_s' and R_b' are independent of the design variable t_j,

$$\frac{\partial g_k}{\partial t_j} = -(L+1)\frac{\partial c_{sk}}{\partial t_j} \tag{36}$$

for shear failure modes, and

$$\frac{\partial g_k}{\partial t_j} = -(L+1)\frac{\partial c_{bk}}{\partial t_j} \tag{37}$$

for bending failure modes.

The procedure for both cases that the first- and the second-order Ditlevsen upper bounds used is described as follows.

First-Order Upper Bound

By differentiating Eq. (18) with respect to a design variable,

$$\phi(-\beta_s)\frac{-\partial\beta_s}{\partial t_j} = \sum_{k=1}^{24} \phi(-\beta_k)\frac{-\partial\beta_k}{\partial t_j} \tag{38}$$

Since each failure mode depends on one design variable only,

$$\frac{\partial\beta_s}{\partial t_j} = \frac{\phi(-\beta_j)}{\phi(-\beta_s)}\frac{\partial\beta_j}{\partial t_j} \tag{39}$$

Consequently,

$$\frac{\partial^2\beta_s}{\partial t_k \partial t_j} = \frac{-\phi'(\beta_s)}{\phi(\beta_s)}\frac{\partial\beta_s}{\partial t_k}\frac{\partial\beta_s}{\partial t_j} \quad \text{for} \quad k \neq j \tag{40}$$

and

$$\frac{\partial^2\beta_s}{\partial t_k^2} = \left[\phi'(\beta_k)\left(\frac{\partial\beta_k}{\partial t_k}\right)^2 + \phi(\beta_k)\frac{\partial^2\beta_k}{\partial t_k^2} - \phi'(\beta_s)\left(\frac{\partial\beta_s}{\partial t_k}\right)^2\right]\Big/\phi(\beta_s) \tag{41}$$

The derivatives on the right-hand sides of Eqs. (39–41) can be calculated from Eqs. (28–30), (36), and (37).

Second-Order Upper Bound

The sensitivities of β_s, with respect to the design variables can be found by differentiating both sides of Eq. (22). Using the results of the previous section and applying Leibnitze's rule, the following formula was dervied:

$$\frac{\partial \beta_s}{\partial t_l} = \phi(-\beta_l)\frac{\partial \beta_l}{\partial t_l}\Big/\phi(-\beta_s) - \frac{1}{\phi(-\beta_s)}\sum_{k=2}^{24}\left[\frac{\partial \beta_j}{\partial t_l}\phi(\beta_j)\Phi\left(\frac{-\beta_k+\rho_{kj}\beta_j}{\sqrt{1-\rho_{kj}^2}}\right) + \frac{\partial \beta_k}{\partial t_l}\phi(\beta_k)\Phi\left(\frac{-\beta_j+\rho_{kj}\beta_k}{\sqrt{1-\rho_{kj}^2}}\right)\right] \tag{42}$$

where j is the integer that is less than k and maximizes $\Phi_2(-\beta_k, -\beta_j, \rho_{kj})$.

When the second-order Ditlevsen's upper bound is used to approximate the probability of failure, discontinuities of the derivative of the constraint will be encountered due to the maximum (max) operator. An example is depicted in Fig. 2, which shows the probability of failure as a function of a typical design variable t. In part A of the curve the index j, which maximizes the second term of Eq. (22), has one value, and in part C of the curve it has another value. The danger in a discontinuous derivative is that an optimizer typically uses derivatives to estimate the behavior of the objective function and constraints as the design variable changes. When the derivative suddenly changes, that estimate can be very poor. Referring to Fig. 2, the estimate near $t = t_b$ will tend to follow the dashed lines instead of the correct solid lines. Fortunately, because of the nature of the maximum function, such estimates will always be conservative; that is, they overestimate the probability of failure. Such conservative estimates create much less of a problem than if the derivative discontinuity results in unconservative estimates.[20] Although the curve shown in Fig. 2 is concave, it can be easily shown that the preceding contention is valid for convex curve as well.

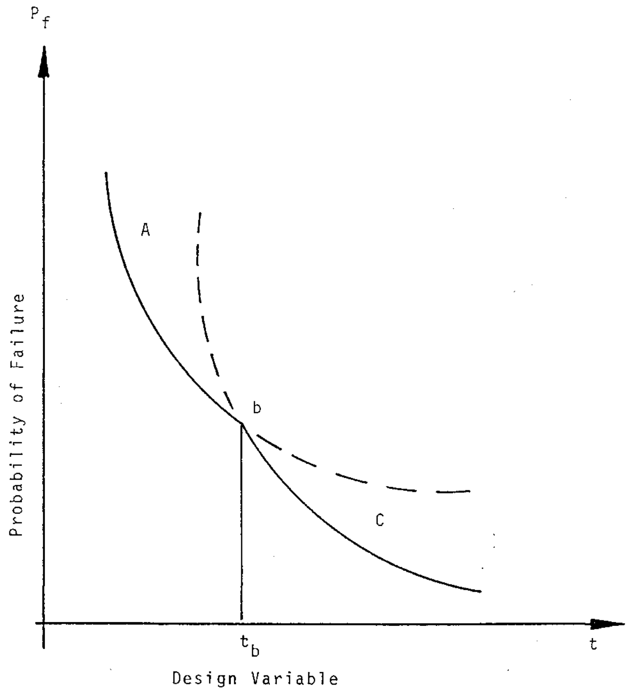

Fig. 2 Discontinuity of constraint derivatives.

Numerical Example

An aircraft wing was optimized deterministically, and it was consequently redesigned using probabilistic optimization. The final designs for the two optimizations were compared in order to assess the advantages of reliability-based optimization.

The computer code NEWSUMT-A (Ref. 21) was used in all optimizations. This program employs a sequential unconstrained minimization procedure that is based on the penalty function method.

Table 1 Data for example aircraft

Design altitude	30,000 ft
Cruising speed	320 mph
Weight	15,000 lb
Wing span	48.73 ft
Wing chord (tip, root)	(2.25, 7.83) ft
Mean chord	5.04 ft
Wing area	279.37 ft^2
Aspect ratio	8.5
Wing loading	53.69 lb/ft^2
Slope of Cl curve	6.094/rad
Air density	0.9312E − 03 slugs/ft^3
Gust speed	41.67 ft/s
Design load factor	3.22
Average material strength:	
Tensile strength	48,000 psi
Shear strength	27,710 psi
Deterministic design values (85% of average values):	
Tensile strength	40,800 psi
Shear strength	23,554 psi

Model Aircraft

A small commuter airplane similar to the Cessna Conquest was selected as a model for our study. The data for this aircraft, which have also been used in Ref. 13, are shown in Table 1. The dimensions of the box beam representing the aircraft wings are presented in Table 2.

In this study the design load factor controls the deterministic optimization of the wings. The design load factor is the maximum value of the limit maneuvering load factor and the limit load factor corresponding to gust loads. The former is to be decided by the designer. The latter can be evaluated using the procedure recommended in the FAA regulations (sections 25–341). The design load factor was found to be 3.22. The details for determining the gust load factor are described in Ref. 13.

Deterministic Wing Design

The wing design must be based on a load factor of 4.83 since FAA regulations prescribe a safety factor of 1.5. The lift distribution was obtained by using Schrenk's[22] method. The optimization problem was formulated as follows.

Minimize the weight of the wing:

$$W = \sum_{i=1}^{12} 2\bar{\rho}s(b_i t_{1i} + h_i t_{2i}) \tag{43}$$

Table 2 Box beam dimensions

Segment no.	Width, in.	Length, in.	Height, in.
1	16.20	24.36	2.70
2	19.55	24.36	3.26
3	22.90	24.36	3.82
4	26.24	24.36	4.37
5	29.59	24.36	4.93
6	32.94	24.36	5.49
7	36.29	24.36	6.05
8	39.64	24.36	6.61
9	42.98	24.36	7.16
10	46.33	24.36	7.72
11	49.68	24.36	8.28
12	53.03	24.36	8.84

Design variables are the thickness of the flanges and the webs.
The constraints are as follows:

$$s_{bi} < s_1 \quad \text{for} \quad i = 1, \ldots, 12 \tag{44}$$

$$s_{si} < s_2 \quad \text{for} \quad i = 1, \ldots, 12 \tag{45}$$

where s_1 is the design material tensile strength, and s_2 is the design material shear strength.

The design strengths were obtained by reducing the corresponding average values by 15% to account for their variability.

The results are shown in Table 3. All of the constraints were active. Furthermore, the flanges are heavier than the webs, which indicates that the bending stress constraints dominate in deterministic optimization.

System Reliability Optimization

In order to compare the deterministic optimization results with the probabilistic optimization counterparts, we designed two wings that have the same reliability and the same weight, respectively, as the design obtained by deterministic optimization. It was assumed the coefficients of variation of bending strength and shear strength are 5% and 10% respectively.

In this study six cases with different correlation coefficients ρ between failure modes were considered in order to investigate how they influence the optimal design. The values of these coefficients are shown in Table 4.

In case I modes corresponding to failure in shear have the same correlation as modes corresponding to bending failure. In case II failure modes in bending have stronger correlation than failure modes in shear. In case III, failure modes in shear have stronger correlation than failure modes in bending. Finally, in cases IV–VI the wing was assumed to be composed of three plates. The failure elements on the same plate were assumed to have higher correlation coefficients than those that lie on different plates.

Discussion of Results

The results are shown in Tables 5–8. Tables 5 and 6 correspond to case I. Comparing the results in Tables 5 and 6 with those from deterministic design (Table 3), we observe that, in both minimum weight and maximum safety optimization, material was transferred from the flanges to the webs. Furthermore, the optimizer increases weight and therefore the safety of light-weight elements, such as the elements near the tip. These trends were also observed and explained in Ref. 13.

Indeed, in minimum weight optimization the percentage of weight change in the flange ranged from a 13.6% reduction at the root to a 9.1% increase at the tip. The percentage of weight increase in the web ranged from 28.6% at the wing tip to 7.9% at the root. The total weight saving was 9.9% of the weight of the deterministic design. In the maximum safety design the percentage of weight change in the flange ranged from a 10.7% increase at the tip to a 3.6% decrease at the root. The percentage of weight increase for the web ranged from 35.7% at the wing tip to 22.2% at the root. The safety index of the wing system increased from 3.099 to 3.81.

Table 3 Deterministic optimal design

	Thickness, in.		Weight, lb	
Segment no.	Flange	Web	Flange	Web
1	0.009	0.010	0.75	0.14
2	0.027	0.020	2.76	0.35
3	0.049	0.030	5.87	0.59
4	0.072	0.038	9.95	0.88
5	0.095	0.046	14.86	1.19
6	0.118	0.053	20.51	1.54
7	0.140	0.060	26.83	1.90
8	0.161	0.066	33.75	2.30
9	0.182	0.072	41.23	2.71
10	0.201	0.077	49.21	3.14
11	0.220	0.082	57.66	3.59
12	0.238	0.087	66.54	4.06

Optimal weight: 352.5 lb
Safety index: 3.099

Table 4 Correlation coefficients between failure modes

	Failure modes					
Case	Bending-Bending		Shear-Shear		Bending-Shear	
I	$0.8^{\|i-j\|}$ [a]		$0.8^{\|i-j\|}$		$0.8(0.8^{\|i-j\|})$	
II	$0.9^{\|i-j\|}$		$0.7^{\|i-j\|}$		$0.6(0.6^{\|i-j\|})$	
III	$0.7^{\|i-j\|}$		$0.9^{\|i-j\|}$		$0.6(0.6^{\|i-j\|})$	
	A[b]	B[b]	A	B	A	B
IV	0.9	0.7	0.9	0.7	0.9	0.7
V	0.9	0.7	0.7	0.5	0.5	0.4
VI	0.7	0.5	0.9	0.7	0.5	0.4

[a] The variables i and j are segment numbers.
[b] A and B refer to failure of elements lying at the same or at different plates, respectively.

The superior performance of the reliability-based optimization can be explained by the following argument. In the system reliability optimization the designer specifies only the overall safety level of the structure. The optimizer is free to determine the best combination of safety levels of the individual components in such a way that the requirement of the overall safety is satisfied. This allows optimal distribution of material. In contrast, when deterministic optimization is used, a minimum safety level for each structural component is prescribed by the designer. These safety requirements are determined empirically. The designer hopes that satisfaction of these requirements implies an acceptable overall safety level. As a result, the search for the optimum is confined by the constraints reflecting these arbitrarily imposed requirements and can be expected to yield suboptical designs.

Obviously, the preceding contention is based on the assumption that all failure modes of a system can be identified. If this is not possible, we must impose additional constraints, probabilistic or deterministic, on elements that are critical for the safety of the system. Even for this case, consideration of system reliability is likely to improve the design.

As can be observed, there is always some uncertainty in the material strength due to fabrication defects, fatigue, residual stresses, and corrosion. Moreover, the level of uncertainty in the material strength varies along the structure. For example, the uncertainty associated with the strength of the elements carrying primarily shear loads is higher than that of elements carrying primarily bending loads. This nonuniform variation in the material strength should be accounted for in the design. In our deterministic design example the uncertainty in the strength was ignored. As a result, material was wasted in overdesigning the flanges, whose strength is less uncertain than that of the webs. On the other hand, the webs were underdesigned because the relatively high coefficient of variation in their strength is not accounted for. Consequently, the distribution of material in deterministic design was substantially different from the actual optimal. In probabilistic design the variation in the strength was taken into account. As a result, material was transferred from the flanges to the webs, and the final design was dramatically improved.

Table 7 compares the safety indices corresponding to the 24 failure modes for the deterministic and minimum weight probabilistic design. The first 12 failure modes refer to flanges with the first corresponding to the tip. The rest correspond to the webs. It can be observed that in deterministic design the safety indices are same for all of the 12 bending stress failure modes as well as for all of the 12 shear stress failure modes. However, the former are significantly higher than the latter.

Table 5 Minimum weight probabilistic optimal design

	Thickness, in.		Weight, lb	
Segment no.	Flange	Web	Flange	Web
1	0.010	0.013	0.82	0.18
2	0.027	0.024	2.74	0.41
3	0.046	0.034	5.60	0.69
4	0.067	0.045	9.31	1.03
5	0.088	0.054	13.70	1.40
6	0.108	0.061	18.71	1.77
7	0.126	0.068	24.21	2.16
8	0.144	0.073	30.18	2.53
9	0.161	0.078	36.48	2.96
10	0.177	0.084	43.21	3.44
11	0.191	0.089	50.16	3.90
12	0.205	0.094	57.48	4.38
Optimal weight: 317.5 lb				
Safety index: 3.092				

Table 6 Maximum safety probabilistic optimal design

	Thickness, in.		Weight, lb	
Segment no.	Flange	Web	Flange	Web
1	0.010	0.014	0.83	0.19
2	0.029	0.027	2.95	0.46
3	0.051	0.039	6.15	0.78
4	0.074	0.049	10.25	1.14
5	0.097	0.059	15.11	1.53
6	0.119	0.067	20.63	1.95
7	0.140	0.075	26.74	2.40
8	0.160	0.082	33.37	2.87
9	0.178	0.089	40.46	3.37
10	0.196	0.095	47.99	3.88
11	0.213	0.101	55.90	4.41
12	0.229	0.106	64.16	4.96
Safety index: 3.81				
Weight: 352.3 lb				

In probabilistic design the safety indices decrease from the wing tip to the root for both bending and shear stress failure modes. With the exception of two stations near the tip, the safety indices of the shear stress failure modes are all larger than those of the bending stress failure modes. Compared with the deterministic design, it can be observed that, except for the station at the tip, the safety indices of the bending stress failure modes decrease, whereas those of the shear stress failure modes increase. This indicates that material has been transferred from the flanges to the webs. The changes in the safety indices in the probabilistic design compared with the deterministic design can be explained with the aforementioned two trends in distributing material by the optimizer. Since the flanges are heavier than the webs at the optimum, their safety levels must be lower than those of the latter. On the other hand, since both the flanges and the webs near the root are heavier than those near the tip, the safety indices must be lower there. Therefore, material was transferred from the flanges to the webs, and the safety indices corresponding to bending stress failure modes were reduced.

The results in Table 8 have been obtained from the following procedure. The reliability of the deterministic optimal design (Table 3) was evaluated by using the first- and second-order Ditlevsen bound for cases I–VI. The estimated safety indices are presented in this table. Consequently, for each of cases I–VI, the wing was designed probabilistically under the constraint that it has the same reliability with the deterministically designed wing. The first-order Ditlevsen bound gives the same results for all six cases because it neglects the correlation between failure modes. Therefore, one design that is the same for all six cases is given for the first-order Ditlevsen bound.

The following can be observed in Table 8:

1) The optimization results from using first- and second-order bounds are the same whenever the correlation coefficient between bending and shear failure modes are identical over the wing (case I). Note that this is true regardless of the value of the correlation coefficient.

2) Whenever the correlation coefficients between bending failure modes are higher than those between shear failure modes, the results from second-order bound optimization are always better than those from the first-order bound optimization in terms of weight savings. As a conclusion, the correlation between failure modes may be important to optimization in a stochastic environment and should be accounted for.

The preceding observations can be explained as follows. The contribution of the bending failure modes to the system failure probability decreases when the correlation coefficients between bending failure modes increase, whereas those between shear failure modes remain constant. In other words, the system is less likely to fail due to excessive bending than due to excessive shear stress. Therefore, the high correlation

Table 7 Individual safety indices of deterministic and minimum weight probabilistic design

	Safety indices	
Mode	Deterministic	Probabilistic
1	$0.445E+01$	$0.505E+01$
2	$0.445E+01$	$0.440E+01$
3	$0.445E+01$	$0.414E+01$
4	$0.445E+01$	$0.403E+01$
5	$0.445E+01$	$0.394E+01$
6	$0.445E+01$	$0.387E+01$
7	$0.445E+01$	$0.381E+01$
8	$0.445E+01$	$0.375E+01$
9	$0.445E+01$	$0.369E+01$
10	$0.445E+01$	$0.365E+01$
11	$0.445E+01$	$0.359E+01$
12	$0.445E+01$	$0.355E+01$
13	$0.379E+01$	$0.485E+01$
14	$0.379E+01$	$0.462E+01$
15	$0.379E+01$	$0.457E+01$
16	$0.379E+01$	$0.454E+01$
17	$0.379E+01$	$0.450E+01$
18	$0.379E+01$	$0.445E+01$
19	$0.378E+01$	$0.438E+01$
20	$0.378E+01$	$0.424E+01$
21	$0.378E+01$	$0.420E+01$
22	$0.378E+01$	$0.419E+01$
23	$0.378E+01$	$0.417E+01$
24	$0.378E+01$	$0.414E+01$
System safety index	$0.3099E+01$	$0.3092E+01$

Table 8 Effect of correlation coefficient

Type	Weight, lb	Safety indices
Deterministic	352.5	
Probabilistic (first-order bound)	317.5	3.092
Probabilistic (second-order bound)		
I	318.9	3.154
II	312.1	3.124
III	325.6	3.211
IV	318.0	3.202
V	311.0	3.104
VI	317.9	3.104

Table 9 Efficiency comparison

	Level III FOFD	AFOSM FOAN	AFOSM SOAN	AFOSM FOFD
obj	170	226	228	366
dobj	10	20	21	15
g	298	41	43	605
dg	0	20	21	0
apg	124	185	185	135
CPU Time, s	315.48	7.20	12.53	106.73
Weight, lb	316.9	317.5	318.9	318.8

FO, first-order bound; SO, second-order bound; FD, finite-difference-evaluated gradients; AN, analytically evaluated gradients; obj, times of objective function evaluations; dobj, times of objective function gradients evaluations; g, times of constraint evaluations; dg, times of constraint gradients evaluations; apg, times of approximate constraint evaluations.

coefficients between bending failure modes will enhance the low coefficient of variation effect of the tensile strength described earlier. For this case the deterministic optimum is even farther away than the actual optimum, and the weight savings from reliability optimization is higher than that for case I.

In order to compare efficiencies of the various optimization approaches, the entire process was repeated using the level III method. The second-moment method was also repeated using a finite-difference method in calculating the derivatives of the constraints. The results and corresponding CPU time with the IBM/3090 system from different methods are summarized in Table 9.

The evaluation of the constraint associated with probability of failure was the most expensive part in the optimization. Therefore, the computational time increases as the number of times that the constraint is evaluated increases. It was observed in Table 9 that the level III method requires the highest number of constraint evaluations, since the gradient calculation was performed with finite-difference method. Furthermore, it uses numerical integration to evaluate the constraints. Therefore, it corresponds to the highest computational time. The AFOSM is significantly more efficient because it does not use nested numerical integration and evaluates constraint derivatives semianalytically.

The design study was repeated for various safety factors ranging from 1.3 to 1.8. The results, summarized in Figs. 3 and 4, show that both the weight savings given the failure probability and the reduction in the failure probability given the weight increase with increasing the prescribed safety factor of the deterministic design.

The difference between the levels of uncertainty in the bending and shear strength is expected to affect substantially the results of probabilistic design and consequently the improvement in the safety or weight of the final design. Therefore, it is interesting to investigate the influence of the coefficients of variation of the axial and shear strength to the weight savings obtained from probabilistic design. For this purpose we redesigned the wing for different levels of the coefficient of variation in the shear strength by employing the minimum weight formulation. The coefficient of variation of the bending strength was fixed at 10%, whereas the coefficient of variation of the shear strength took values in the range of 5–15%.

The weight reduction as a percentage of the weight of the deterministic design is plotted in Fig. 5 as a function of the ratio of the coefficients of variation of shear and bending strength. The improvement in the weight increases monotonically with the coefficient of variation of the shear strength. This observation can be easily explained by accounting for the trends of the optimizer to transfer material from elements with low coefficient of variation in their strength to elements with high uncertainty in their strength.

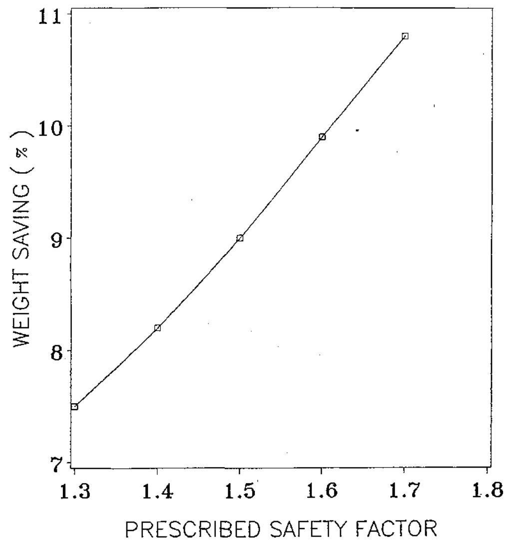

Fig. 3 Weight savings vs safety factor.

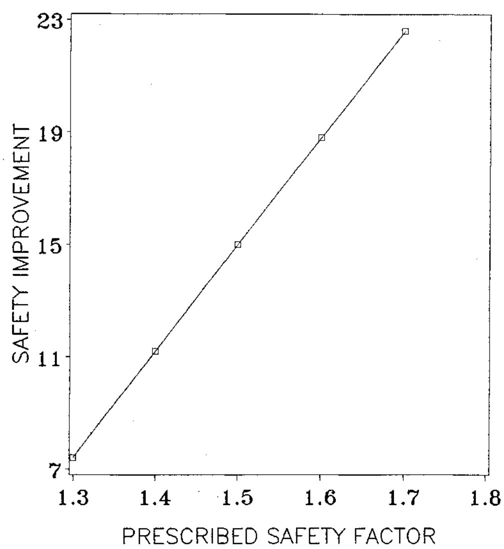

Fig. 4 Safety improvement vs safety factor.

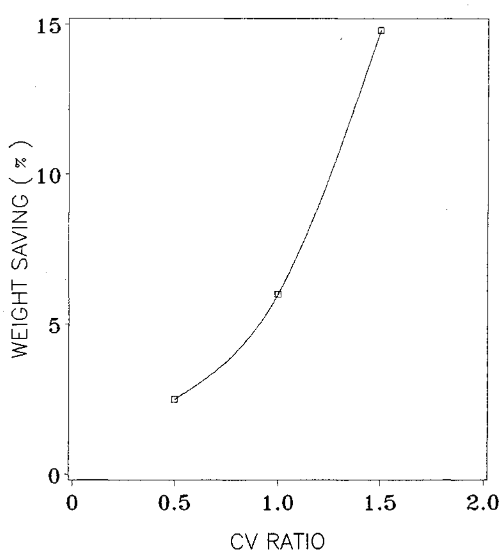

Fig. 5 Weight savings vs CV ratio [CV ratio = CV (shear strength)/CV (tensile strength)].

Conclusions

The main conclusions from our study are given as follows:

1) System reliability based optimization can be used to design safer and cheaper aircrafts.

2) In probabilistic design it is better to employ the AFOSM method than the level III method, to assess structural safety.

3) The correlation between failure modes of a structural system might be important in system reliability based design.

4) In our opinion the easiest way to account for the statistical correlation between failure modes in estimating system reliability is to use the second-order Ditlevsen's bounds. In that case a problem that may be encountered is associated with the discontinuity of the derivatives of system reliability with respect to the design variables. It was shown that, if a penalty function method is used in optimization, this problem is circumvented.

The wing model that was used in this study is too simple compared to wing models employed in real-life design situations. In principle, the proposed design procedures are applicable to real-life complex models. For such cases the stochastic finite element method[23] can be employed to estimate reliability. However, the computational cost for reliability-based design will be prohibitively high. Consequently, it is important to improve the efficiency of reliability optimization. Further research efforts, such as the one presented in Ref. 24, should be directed toward this goal.

Acknowledgment

The authors thank R. T. Haftka for his comments on this paper.

References

[1]Code of Federal Regulations No. 14, Aeronautics and Space, Pt. 25, 1988.

[2]Thoft-Christensen, P., and Murotsu, Y., *Application of Structural System Reliability Theory*, Springer-Verlag, Berlin, 1986.

[3]Moses, F., and Kinser, D. E., "Optimum Structural Design With Failure Probability Constraints," *AIAA Journal*, Vol. 5, June 1967, pp. 1152–1158.

[4]Thoft-Christensen, P., and Sorensen, J. D., "Reliability Analysis of Elasto-Plastic Structures," *Proceedings of the 11th IFIP Conference on System Modeling and Optimization*, Springer-Verlag, Berlin, 1984, pp. 556–566.

[5]Sorensen, J. D., and Thoft-Christensen, P., "Structural Optimization with Reliability Constraints," *Proceedings of the IFIP 12th Conference on System Modeling and Optimization*, Springer-Verlag, Berlin, 1986, pp. 876–885.

[6]Feng, Y. S., and Moses, F., "A Method of Structural Optimization Based on the Structural System Reliability," *Journal of Structural Mechanics*, Vol. 14, No. 4, 1986, pp. 437–453.

[7]Feng, Y. S., and Moses, F., "Optimum Design, Redundancy and Reliability of Structural Systems," *Computers and Structures*, Vol. 24, No. 2, 1986, pp. 239–251.

[8]Frangopol, D. M., "Interactive Reliability-Based Structural Optimization," *Computers and Structures*, Vol. 19, No. 4, 1984, pp. 559–563.

[9]Frangopol, D. M., "Sensitivity of Reliability-Based Optimum Design," *Journal of Structural Engineering*, Vol. 111, No. 8, 1985, pp. 1703–1721.

[10]Rao, S. S., "Automated Optimum Design of Wing Structures: a Probabilistic Approach," *Computers and Structures*, Vol. 24, No. 5, 1986, pp. 799–808.

[11]Hajela, P., and Bach, C. T., "Optimal Structural Sizing for Gust Induced Response," *Proceedings of the AIAA/ASME/ASCE/AHS/ASC 29th Structures, Structural Dynamics nad Materials Conference*, 1988.

[12]Hajela, P., and Bach, C. T., "Optimal Structural Sizing for Gust Induced Response," *Journal of Aircraft*, Vol. 26, No. 4, 1989, pp. 395–397.

[13]Yang, J. S., Nikolaidis, E., and Haftka, R. T., "Design of Aircraft Wings Subjected to Gust Loads: a First Order Second Moment Approach," *Computers and Structures*, Vol. 36, No. 6, 1990, pp. 1057–1066.

[14]Nikolaidis, E., and Burdisso, R., "Reliability Based Optimization: a Safety Index Approach," *Computers and Structures*, Vol. 28, No. 8, 1988, 781–788.

[15]Sherman, D. J., "The Effect of Spanwise Gust Variations on the Transfer Function of an Aircraft Model With One Degree of Freedom," ARL Structures Note 431, 1976.

[16]Wu, Y. T., and Wirsching, P. H., "New Algorithm for Structural Reliability Estimation," *Journal of Engineering Mechanics*, Vol. 113, No. 9, 1987, pp. 1319–1336.

[17]Rosenblatt, M., "Remarks on a Multi-Variate Transformation," *Annals of Mathematical Statistics*, Vol. 23, 1952, pp. 470–472.

[18]Ditlevsen, O., "Narrow Reliability Bounds for Structural Systems," *Journal of Structural Mechanics*, Vol. 7, 1979, pp. 453–472.

[19]Sorensen, J. D., "Reliability Based Optimization of Structural Systems," *Proceedings of the IFIP 13th Conference on System Modeling and Optimization*, 1987.

[20]Starnes, J. H., Jr., and Haftka, R. T., "Preliminary Design of Composite Wings for Buckling Stress and Displacement Constraints," *Journal of Aircraft*, Vol. 16, 1979, pp. 564–570.

[21]Grandhi, R. V., Thareja, R., and Haftka, R. T., "NEWSUMT-A: A General Purpose Program for Constrained Optimization Using Constraint Approximations," *Journal of Mechanisms, Transmission and Automation in Design*, Vol. 107, 1985, pp. 94–99.

[22]Schrenk, O., "A Simple Approximation Method for Obtaining the Spanwise Lift Distribution," NACA TM-1910, 1940.

[23]Cruse, T. A., Wu, Y. T., Dias, B., and Rajagopal, K. R., "Probabilistic Structure Analysis Methods and Applications," *Computers and Structures*, Vol. 30, No. 1/2, 1988, pp. 163–170, 316–322.

[24]Maglaras, G. K., "Integrated Analysis and Design in Stochastic Optimization," MS Thesis, Virginia Polytechnic Institute and State University, Blacksburg, VA, 1989.